Enhancing Offshore Wind Turbines Performance with Hybrid Control Strategies Using Neural Networks and Conventional Controllers

Eduardo Muñoz-Palomeque[1,*], J. Enrique Sierra-García[1] and Matilde Santos[2]

[1] Digitalization Department, University of Burgos, Burgos, Spain
[2] Institute of Knowledge Technology, Complutense University of Madrid, Madrid Spain
∗ Corresponding author. emp1016@alu.ubu.es, jesierra@ubu.es

Abstract

A wind turbine is a complex energy converter that requires a robust control solution to overcome performance limitations caused by its mechatronics and external disturbances. Within the turbine operation regions, in the area below the nominal power, the challenge of achieving a precise and highly efficient response must be addressed using multi-objective control strategies that can also contribute to the stability of the structure, reducing vibrations. In this work, a control architecture to maximize the power generation and minimize the vibrations is proposed. Based on this architecture four different hybrid control strategies exploiting radial basis function neural networks and conventional regulators are proposed to cover this twofold objective. The controllers calculate the appropriate electromagnetic torque to track the maximum power point and thus achieve the generation of maximum power, while reducing the acceleration of the tower movement. The neural controllers use a non-supervised learning algorithm to adaptively adjust the weights of the neuros to better couple to the wind turbine dynamics. These combined control methods are tested on a 5 MW floating offshore wind turbine under the influence of winds and waves. The results show that these hybrid strategies are valid for achieving a more efficient response and decreasing turbine fatigue, thus extending their lifetime.

Graphical abstract

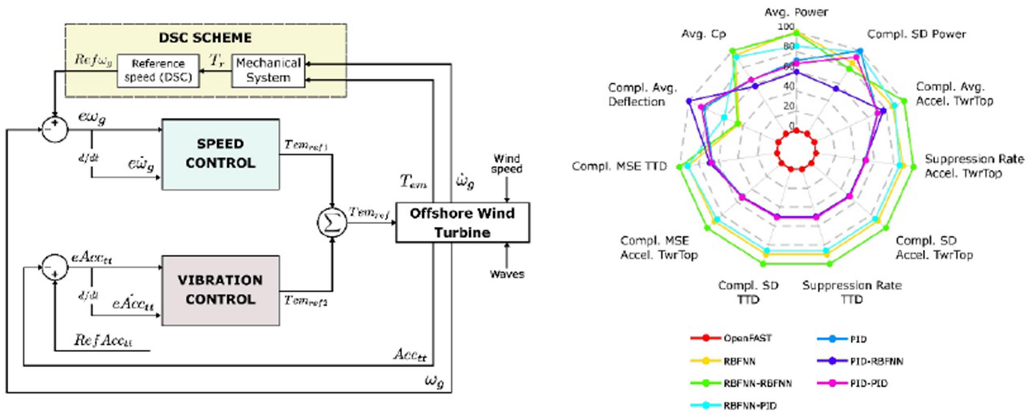

Keywords: Hybrid control, PID, Neural Networks, Floating Offshore Wind Turbine, Vibration

Highlights

- A general control architecture to maximize power generation and minimize vibrations in FWOT is proposed.
- Following this architecture four different hybrid controllers are implemented: ANN-PID, PID-ANN, ANN-ANN and PID-PID.
- Methodology to optimize these hybrid controllers based on metaheuristic techniques.
- Comparison of hybrid controllers based on power and vibration KPIs and identification of the best performance.
- Hybrid controllers outperform the performance of openFast embedded controller providing larger power and smaller vibrations.

1. Introduction

Renewable energy is proving to be a successful alternative to address the environmental problems caused by other widely used energy sources, based on fossil fuels, with polluting and negative effects on the environment and climate change (Kadri, Marzougui and Bacha 2019; Salih, Nawafal and Hamoodi 2023). In addition, these energy sources help to solve the need for greater energy production in society, which is a fact when observing the growth of populations, machines, industries, and the large number of devices that have become part of our lives. The transition towards sustainable sources with less harmful repercussions for the planet and its living organisms, including human health and climate change, encourages the advancement and exploitation of clean energy sources.

In this category of sustainable technologies, wind turbines are an important player with rapid growth. Their natural resource, wind, abundant in most countries, and other benefits such as being a mature technology, cost, environmental friendliness, and high energy output make wind converters very suitable devices for the production of electric power. Due to these advantages, onshore wind turbines have been extended to offshore wind turbine technology, taking advantage of the wide coastal and oceanic areas, and favourable orographic conditions for energy extraction (Zhou et al., 2023).

The operational response of a wind turbine can be divided into zones according to the wind speed range. The maximum power point tracking (MPPT) region is an essential stage. This region is characterized by working at a wind speed below the nominal value, according to the capabilities of the device, where the pitch angle of the blades is not controlled. In this zone, maximum power production is necessary for the system to achieve the highest possible energy conversion and reach its nominal value. To achieve this, the rotation of the hub, linked to the generator, must satisfy a non-linear relationship with the electromagnetic torque. Controlling these variables allows the systems to produce the appropriate power.

For the correct operation of these complex and non-linear energy devices, control is essential and must be studied in depth. Improving the efficiency of energy conversion is key to reducing costs. For this reason, controllers have evolved from simple techniques for regulating specific variables to more sophisticated and intelligent approaches that develop multi-objective methodologies. In offshore converters, the controller must also deal with disturbances and variability in the environment, since in addition to the wind, the turbine is subject to waves and currents. These disturbances reduce energy efficiency and cause an increase in stress and vibrations in the structure of the wind turbine (López-Romero and Peñas, 2023; Aboutalebi et al., 2022).

With this approach in mind, this research study aims to examine the control in the MPPT region of a wind turbine while reducing the vibrations. To do it a general control architecture designed to maximize the power generation and minimize the vibrations is proposed. Based on this general architecture, different hybrid control architectures are designed exploiting neural networks and conventional PID (Proportional-Integral-Derivative) regulators, optimized by means of evolutionary heuristic techniques, genetic algorithms (GA).

They have been applied to a 5 MW floating offshore wind turbine. A comparative analysis of various controller combinations is carried out with a double objective: to achieve maximum efficiency and at the same time reduce structural vibrations in the wind turbine. The main strategy is based on the regulation of the electromagnetic torque, which is modified according to the speed of the generator and the acceleration of the tower movement. The weights of the neural networks are updated while the system is working by an unsupervised learning algorithm which considers the power and the vibrations. Therefore, in this approach, labelled data are not needed to train the networks. KPIs covering both aspects have been defined to measure the efficiency of the different control solutions proposed. This allows identifying the strengths and limitations of the control techniques and finding the best hybrid solution. These proposals are compared with each other and with the speed-torque control implemented in the OpenFAST reference simulator used as a benchmark.

The main contributions can be summarized as follows:

- A general control architecture that deals with a double control goal commonly addressed separately referred to maximize power generation and minimize vibrations in a Floating Offshore Wind Turbine (FOWT) is proposed.
- Following this architecture four different hybrid controllers are implemented: RBFNN-PID, PID-RBFNN, RBFNN-RBFNN and PID-PID.
- The ability of neural controllers to reduce fore-aft vibrations by torque action has been explored.
- Methodology to optimize these hybrid controllers based on metaheuristic techniques.
- Comparison of hybrid controllers based on power and vibration KPIs and identification of the best performance.

- Application of an adaptive neural network approach for increasing the performance of the control system by learning the changing conditions in the control scenario with an unsupervised capability of execution.

This article is organized as follows: Section II presents a brief literature review on MPPT control techniques. Section III defines the control problem, contextualizing some important concepts of wind turbines such as the operational zones. The hybrid control architecture is introduced in Section IV, describing the controllers used in this research. The results of the hybrid control strategies are then presented and compared, analysing the contribution of each configuration in energy production and vibration reduction. The work ends in Section VI with conclusions and future work in this line of research.

2. Works related to Maximum Power Point Tracking control of FOWTs

Power generation in wind turbines, and specifically in the MPPT region, is a problem that has interested control engineering researchers for decades due to the challenges presented by their dynamics and the disturbances to which they are exposed, especially marine ones. In the literature on MPPT control, classical approaches have been the basis for future innovations. Some examples are tip speed ratio (TSR) control, direct speed control, indirect speed control, power signal feedback (PSF) and disturbance and observation (P&O) control, which are predecessors of other more robust algorithms widely used in wind turbine control, such as neural networks and fuzzy logic (Salic et al. 2019).

Hybrid control proposals are also found in this field to increase the effectiveness of final control, where a wide variety of techniques are used (Eduardo Muñoz-Palomeque, Sierra-García and Santos 2023b). Some works focused on advanced control strategies are the following.

In (Atallah et al. 2022), the TSR control principle is used to maximize aerodynamic power. This approach is developed by adding an estimator of the wind speed with an adaptive gain sliding mode control (AG-SMC). In (Mahmoud et al. 2022), optimal torque control (OTC) is implemented in the machine-side converter of the wind turbine, complemented by a FLC that replaces the classic PI controller to increase the performance of the system when speed changes occur. The Perturb and Observe technique is applied in (Gouabi et al. 2021), where the classic approach is modified by an FLC controller, which is incorporated to attain an adaptive step size in the algorithm. This strategy also presents modifications in the literature. In (Khan 2022) the authors use the P&O control to generate the optimum duty cycle for better power tracking. A fuzzy controller is used to estimate the optimum perturbation sent as the input to the P&O algorithm.

A specific intelligent technique, neural networks, has been also selected for MPPT wind turbine control purposes (Chetouani et al. 2023). These intelligent control methods bring a useful advantage: they can analyse and learn from the data and provide an excellent projection of the new input as the output to the system (Villegas-Mier et al. 2021). A backpropagation neural network is proposed in (Korlepara and Subramani 2022) to estimate the reference power in a wind energy system. In order to track the maximum power point of the wind turbine and then enhance its performance, in (Penta, Venkateshwarlu, and Sujatha 2023) a hybrid controller using a dynamic evolving neuro-fuzzy system in conjunction with a fire hawk optimizer is designed. Neural networks have been combined with reinforcement learning (RL) algorithms to control the power production of wind turbines in (Liu et al. 2020; Pinto, Deltetto, and Capozzoli 2021). In (Arianborna, Faiz, and Erfani-Nik 2023) the authors propose an MPPT controller based on the integration of the Q-learning strategy and strengthened by a deep neural network to define the policy for the Q-learning algorithm.

Radial basis function is another approach of intelligent neural controller that is used in wind turbine MPPT control (E. Muñoz-Palomeque, Sierra-García, and Santos 2023a). Using the radial basis function neural network (RBFNN) and the d-axis stator current control strategy, an MPPT controller is formulated in (Anh Nguyen et al. 2021), which demonstrates that the neural controller-based approach is adequate to track the maximum power in a wind turbine system. An offline training RBFNN complemented by a PID controller is proposed in (Rahman and Rahim 2020) to reach the maximum power point from the power and rotor speed inputs.

Furthermore, linking the MPPT problem to the idea of structural vibration and dynamic load mitigation in wind turbines, this study is commonly cover as a particular topic. Active Generator Torque Control (AGTC) is an extended method in this area that is not frequent in floating offshore wind turbines. There are some applications in bottom-fixed offshores turbines, like in (Lara et al., 2023a). In this paper, an AGTC approach is described to reduce lateral tower fatigue within the nominal zone of a monopile offshore WT. The same authors propose in (Lara et al., 2023b) a control based on a collective pitch combined with two active tower damping controls, one for frontal oscillations and another for lateral displacements, which produces an additional component of the generator torque. Again, for a monopile offshore WT an active torque controller is proposed in (Wang L. et al., 2024), reaching a relevant reduction of side-to-side dynamic loading of a 10 MW bottom-fixed WT at the cost of reducing the annual power production. The paper by (Wang J. et al., 2024) states that few studies have examined the correlation between wind turbine structural vibration reduction and power generation control. To the best of our knowledge this is the first work where neural torque controllers are explored to control the fore-aft vibrations.

In most of the articles the target is the MPPT and the vibrations in the turbine are not considered although it is an important aspect to study. For this reason, in this article we propose a strategy for the combination of controllers and face the MPPT and vibration control simultaneously.

3. Control Problem in Wind Turbines

The dual control objective is both maximum power control and vibration control, largely induced by wind and waves in the case of floating wind turbines, but also as an effect of the control itself.

The control problem for maximum power conversion involves the wind turbine generator, and therefore the linked hub, acquiring a rotation speed as a consequence of the induced torque. Thus, if the wind system moves at an optimal speed, the torque can also reach the desired operating point for maximum electric power generation (Sitharthan et al. 2019). The combination of both variables allows the system to regulate its dynamics to follow the desired behaviour. Because this interaction is non-linear, sensitive to changes and mostly unknown, obtaining the best combination between these variables for each wind condition is difficult.

The induced torque helps the rotational components to increase speed or decelerate, seeking the most efficient ratio that produces the greatest amount of energy, decreasing power losses in the conversion process. Torque, T, and angular speed, ω, are two important variables that are closely related to the power of the wind turbine (Tsai et al. 2022):

$$T = \frac{P}{\omega} \quad (1)$$

Due to the limitations of the components and capacity of the power device, including the mechanical parts and electrical elements, the wind turbine is designed to work in operating zones, depending on the speed of the wind that impacts on the turbine blades. The main objective is to get the maximum performance from the wind, until the force that it exerts on the turbine endangers its safety, and then the rotation of the blades is slowed down or even stopped to avoid structural damage.

Taking these considerations into account, four operating regions of the turbine are defined, depending on the wind speed, which are shown in Figure 1.

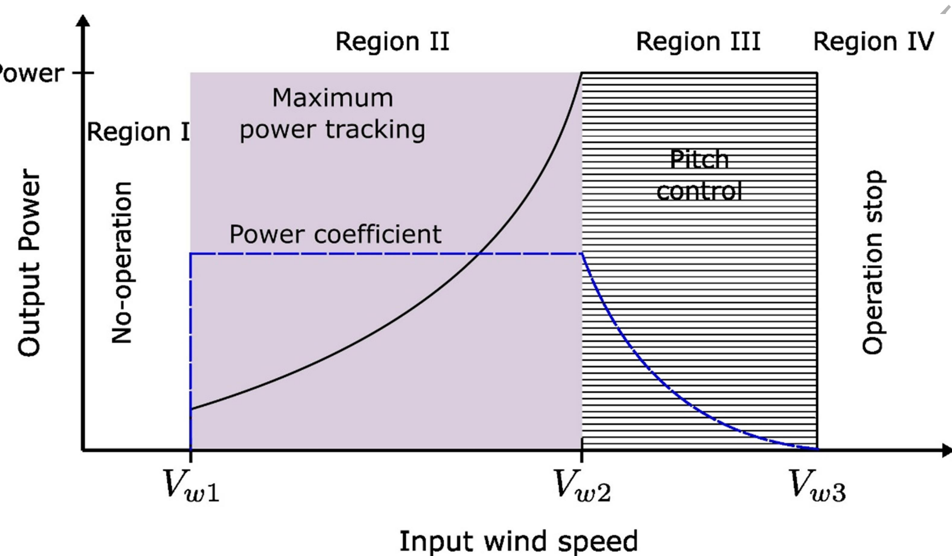

Figure 1. Operating regions of a wind turbine system.

The first region is non-operating, the turbine does not produce energy as the wind speed is low and the force required to start the hub rotation is not sufficient. From the initial wind speed V_{w1}, the turbine enters the MPPT region or Region 2, which ends at the maximum wind speed limit V_{w2}. In this zone the turbine is controlled based on torque to increase its generation up to the maximum power for the different wind speeds. In Region 3 the wind speed exceeds the rated speed V_{w2} and the turbine reaches the rated power of the generator. To avoid damage due to excessive rotation speed and endangering the power generation and the system, the blade pitch control is activated, decreasing the intensities of the incident forces, and maintaining the energy production at its maximum point. When the incoming wind hits too hard, at speeds above V_{w3}, the wind turbine stops its operation to ensure the safety of the entire device (Region 4).

3.1 MPPT Control in Wind Turbines

In the second region of the wind turbine, the MPPT takes place. The control is characterized by the tracking of a specific and increasing power function as the wind speed increases, always below the nominal power generation point. The power curve (Region 2 in Figure 1) is accompanied by another descriptive curve representing the optimum power conversion efficiency. This second curve is called the optimal power coefficient ($\hat{C}_p$), with specific values for each turbine (Figure 1, blue line). This curve reaches a maximum value and is maintained throughout the entire region. However, the power coefficient effectively experimented by the wind turbine (WT) depends on the ratio between the velocity of the blades and the wind velocity. Therefore, in the MPPT region the objective of the controller is to regulate the velocity of the blades to follow the optimum curve, thus, to make the power coefficient to follow its optimum value, $\hat{C}_p$. This ideal behaviour allows the system to maximize the power conversion.

The wind energy hitting the wind turbine is captured through the rotation of the blades. The captured power is expressed in (2) (Chetouani et al. 2023) and depends on the air density, ρ (Kg/m^3), the wind speed, V_ω (m/s), the length of the blades that delimit the swept area, A (m^2), and finally on the power coefficient, C_p.

$$P = \frac{1}{2}\rho C_p A {V_w}^3 \tag{2}$$

The last term C_p is the result of a nonlinear function between the tip speed ratio, λ, and the pitch angle of the blades, β (°):

$$C_p = f(\lambda, \beta) \tag{3}$$

The tip speed ratio, λ, or TSR (4), is calculated as the division between the linear velocity of the blades and the current wind speed, where ω_r is the rotor speed (rad/s), and R is radius of the rotor, that is, the blade length (m).

$$\lambda = \frac{\omega_r R}{V_w} \quad (4)$$

Additionally, the mechanical part of the wind turbine reflects the transmission of speed and torque. Considering a two-mass wind model (Muñoz-Palomeque et al. 2023a), the mechanics that link the hub and the generator are:

$$\dot{\omega}_r = \frac{\dot{\omega}_g}{N} = \frac{T_r - NT_{em}}{N^2 J_g + J_r} \quad (5)$$

In this equation, T_r is the mechanical torque, T_{em} is the electromagnetic torque, $\dot{\omega}_r$ is the acceleration of the low speed shaft in the hub, which can be expressed in terms of the generator acceleration $\dot{\omega}_g$ as $\dot{\omega}_g/N$. The moments of inertia on the hub side and the generator are J_g, and J_r, respectively, and N is the gearbox ratio that connects the low and high speed shafts.

The MPPT controller regulates the angular rotor speed ω_r by adjusting the T_{em} of the generator (5). This signal modifies the λ according to (4), what in turn updates the C_p, according to (3). This way the C_p is regulated to track the optimum value.

3.2 Structural Vibration Control in Wind Turbines

The vibrations and structural stresses of a turbine have various sources. The wind turbine is a mechatronic composition of huge and heavy elements, interconnected with each other. To perform their work, these parts are in motion, describing rotational displacements. This interaction and the effects of the movements result in the appearance of vibrations. In addition, structural fatigue is related to the wind and, in floating turbines, to sea currents and especially waves, and to the stability of the platform. Furthermore, the effects of MPPT control and pitch control also affect the stability of the wind turbine and the impact of vibrations. These vibrations reduce the life of components and increase maintenance needs, hence the importance of trying to reduce them.

There are several ways to try to reduce them. For example, since the movement of mechanical elements produces these vibrations, they can be attenuated with control strategies that produce smoother movements and a less abrupt system response (Serrano et al., 2022). They can also be mitigated with structural control elements.

When the wind hits the FOWT produces displacements in the tower and the platform. The tower displacement movement can be divided in two components (Figure 2): fore-aft (in the direction of the wind) and side-side (perpendicular to the wind). The fore-aft displacement is also called tower-top displacement (TTD).

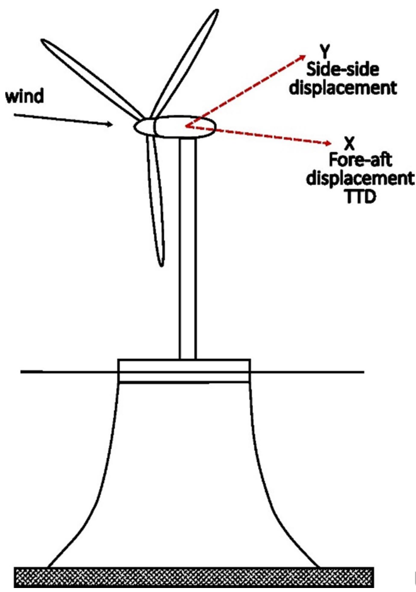

Figure 2. Fore-aft (TTD) and side-side displacements in a floating offshore wind turbine.

The main displacement is produced in the fore-aft direction. Thus, its value, velocity, and acceleration are useful indicators of the movement and the vibrations in the FOWT. Variations in the rotor speed produce forces that can affect these vibrations, thus a good approach is to introduce information of the TTD into the control loop to reduce the effect of the vibrations.

The rotation of the blades produces centrifugal forces. When a blade is aligned with the Y-axis (Figure 2) the centrifugal force produces yaw torque in the toqer. When a blade is aligned with the tower the centrifugal force produces a torque around the Y-axis, what generates fore-aft forces and thus accelerations. The centrifugal force is proportional to the rotor speed and the torque control is used to adjust the rotor speed, therefore the fore-aft acceleration is related with the torque control. Furthermore, previous studies have studied the frequency spectrum of the fore-aft vibrations and have found relations between the frequency components and the rotor speed due to the shadow effect (Serrano-Antoñanazas et al., 2024). Therefore, the speed adjustment done by the torque control also affects the fore-aft vibrations.

4. Architecture of the Hybrid MPPT Controller of the FOWT

A general control architecture for MPPT control of a wind turbine will be proposed. Then the elements of this general control configuration will be replaced by different controllers implemented with different techniques, both conventional and intelligent.

Generating the maximum possible power is a priority for the control action. To achieve this behaviour in the MPPT zone, the generator rotation speed and the electromagnetic torque must be linked. The speed of the machine, also related to the rotation of the turbine, and the electromagnetic torque share a behaviour that is reflected in the non-linear curve representative of each wind device for the entire speed and operating torque range of the turbine. As described by (5) when a higher electromagnetic torque is induced, the rotation speed decreases. This means that the torque acts as a built-in brake, corresponding to an electric brake.

To address this non-linear behaviour in the MPPT stage, a dual controller is designed. On the one hand, the angular speed reference of the generator is established, $Ref\omega_g$, which will be the reference to adjust the torque. In the MPPT operation, the optimal power point is also related to the effective complement between speed and torque. The torque acts as a brake that influences on the wind turbine rotation. The equilibrium of these non-linear variables allows the system to keep the desired speed that tracks the maximum power. This required speed is estimated by the relationship between the mechanical torque that joins the hub and the generator, the electrical torque that is induced in the generator, and some specific constants that determine the operation of the wind system. With this framework, in this study, direct speed control (DSC), expressed in (6), is used as a basis.

$$\tilde{T}_r = \frac{\dot{\omega}_g}{N}\left(N^2 J_g + J_r\right) + N T_{em}, \quad Ref\omega_g = N \cdot \sqrt{\frac{\tilde{T}_r}{K_{opt}}}, \tag{6}$$

In this equation, $\tilde{T}_r$ is an estimation of the rotor torque based on the measured electromagnetic torque T_{em} and the acceleration of the generator, $Ref\omega_g$ is the generator speed reference for maximum power tracking, and K_{opt} is the optimal constant for the specific wind turbine. This gain involves aerodynamic and mechanical characteristics of the system, as expressed in (7). The variables are the air density, ρ, the radius of the rotor, R, and the optimal power coefficient, $\hat{C}_p$, and optimal TSR, $\hat{\lambda}$.

$$K_{opt} = \frac{1}{2}\frac{\rho\pi R^5 \hat{C}_p}{\hat{\lambda}^3} \quad (7)$$

The DSC is a classical control scheme based on the mathematical relationship between different variables of the wind turbine that allows the connection of the power transmission blocks to control the speed of the wind device. This general control is represented in Figure 3.

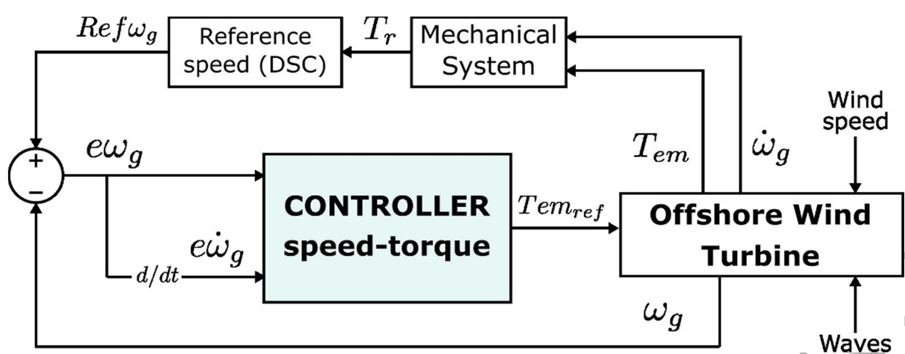

Figure 3. DSC control of a wind turbine.

As can be seen, this control framework requires the implementation of an efficient regulator of the electromagnetic signal. This controller can be as simple as a conventional PID control, an intelligent control solution, or even a synergy of them. It is important to accurately reach the required torque so that the rotation speed is maintained at the desired value and thus maximize energy production. The complexity of the control in this region is given because the relationship between the main variables involved in this methodology, that is, between speed and torque, is unknown.

In addition, the reduction of vibrations in the turbine during this operation will be considered, simultaneously with the extraction of maximum power. For this second objective, the acceleration of the tower, Acc_{tt}, is used as an indicator of the vibration produced in the structure.

Considering the tower acceleration as a manifestation of vibrations, the influence of T_{em} with respect to Acc_{tt} is considered to exist, as a practical way to mitigate vibrations (Golnary and Tse, 2022). In our case, the torque reference is calculated using that acceleration to influence the electrical and mechanical response of the wind system.

That is, the acceleration of the tower top is used to design a controller that complements the task of the MPPT, focusing on attenuating vibrations. This second controller can also be designed with a classical approach or with an intelligent technique. Consequently, a hybrid controller can be implemented to meet this dual objective.

Considering this combined control approach, the hybrid control scheme is presented in Figure 4. The graph shows the three main parts of the controller. It consists of the reference speed estimation within the DSC framework and two complementary controllers, one for the MPPT and the other for vibration mitigation. The union of the output of both controllers is the action used to regulate the wind turbine. Thus, the double objective of maximizing power conversion while attenuating vibrations is achieved, increasing the turbine stability and its efficiency. The connection of these two control ideas conveys a promising reference for extending the WT control matter due to the lack of deep analysis in their mutual relation (Wang J. et al., 2024).

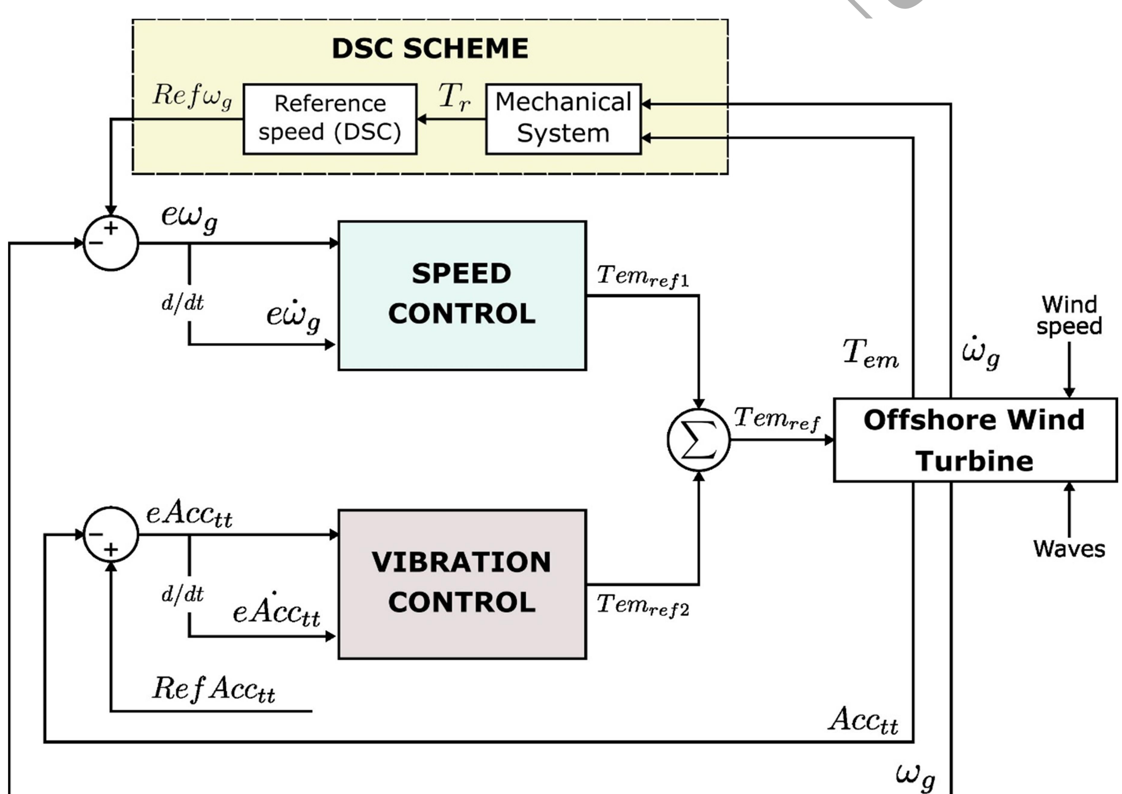

Figure 4. Hybrid controller in the MPPT region of a wind turbine.

In this control scheme, the signals involved are the following. The MPPT controller receives as input the generator speed error variable ($e\omega_g = Ref\omega_g - \omega_g$) and its derivative. The controller then estimates an electromagnetic torque reference as output, Tem_{ref1}.

The input to the vibration controller is the acceleration at the top of the tower. To reduce it, a complementary torque, Tem_{ref2}, is obtained, which is added to the main response of the MPPT, as expressed in (8), where the reference torque to the system, Tem_{ref}, is calculated.

$$Tem_{ref} = Tem_{ref1} + Tem_{ref2} \tag{8}$$

This wind turbine MPPT control architecture is implemented with combinations of neuro control and PID regulators for speed controller and vibration control, this way PID-PID, PID-NN, NN-PID and NN-NN configurations are tested.

4.1 Neural Network Based Controllers for Wind Power Systems

Although the control architecture is general and can be applied for different neural networks, a radial basis function neural network (RBFNN) is selected to be included in the wind turbine control system. This is a robust network option that provides highly accurate outputs and quick control responses (Sitharthan et al. 2019). With this neural network architecture, the use of one hidden layer is necessary, which is an advantage in the design process as it means an extra degree of freedom in the configuration. This neural network can be adapted for both MPPT main control and oscillation damping. Furthermore, RBFNN are low computational demanding, this aspect is key to implement this technique real time controllers such as programming logic controllers.

In this work, the controllers have been implemented as unsupervised learning systems, so they are able to adapt to the changing dynamics during operation of the wind turbine. Then, no previous data were used to train the neural networks. An unsupervised learning algorithm changes the weights of the networks according to the inputs in order to maximize the power an minimize the vibrations.

4.1.1 Neural Control of the generator speed of the FOWT

One option is to include the neural network to regulate the machine torque in the wind turbine speed for the MPPT. This non-linear technique allows to respond and adapt more effectively to the turbine power curve. Using a radial basis function neural network (RBFNN), the radial distance from the pair error speed, $e\omega_g$, and its derivative, $e\dot{\omega}_g$, to the position of the centre of each neuron, c_i, is calculated using the normalized Euclidean distance (9).

$$\left\|\left(e\omega_g, e\dot{\omega}_g, i\right)\right\| = \sqrt{\frac{\left(c_{i1} - e\omega_g\right)^2}{Max\left(e\omega_g\right)^2} + \frac{\left(c_{i2} - e\dot{\omega}_g\right)^2}{Max\left(e\dot{\omega}_g\right)^2}} \tag{9}$$

In the 2D plane where the neurons are distributed, the value c_{i1} corresponds to the coordinate of the *i*-neuron for the $e\omega_g$ dimension and c_{i2} for the $e\dot{\omega}_g$ dimension.

The output of the network, the electromagnetic torque reference, Tem_{ref}, is estimated by solving (10) every control time interval T_c. The action of the RBFNN is calculated as the cumulative product of the weights in the hidden layer and the negative exponential function of the radial distance, calculated for the generator speed errors. The multiplication of the weight the *i*-neuron corresponds to the relationship between the single hidden layer to the output layer. This calculation is performed for each of the neurons in the hidden layer, which have their own variable weight.

$$Tem_{ref1} = \sum_{i=1}^{N_1} W_i \cdot e^{-\left(\frac{\left\|\left(e\omega_g, e\dot{\omega}_g, i\right)\right\|}{\delta_1}\right)} \tag{10}$$

In this expression (10), W_i is the weight of the *i*-neuron, $\|\cdot\|$ is the normalized distance of the inputs and the center of the neurons, the constant δ_1 is the width of the neuron, and N_1 is the number of neurons in the network.

To adapt the results of the neural controller in real time, an unsupervised approach is used, which updates the weights of the neural network. The increment in the weight of the *i*-neuron is described by (11). The speed error and its derivative are used to compute the maximum increment of the weight. As according to (9-10) not all the neurons have the same contribution to the output of the network, but their contribution is modulated by the distance. The closer the neuron the larger the contribution. This distance is also used to modulate the increment of the weight. Really the speed error is combined with its derivative as in an PD controller to compute the maximum increment. The coefficients K_1 and K_2 allow to balance the importance of the error and its derivate in the increment of the weight.

$$\Delta W_i(t) = \mu_1\left[e\omega_g K_1 + e\dot{\omega}_g K_2\right] \cdot e^{-\left(\frac{\|(e\omega_g, e\dot{\omega}_g, i)\|}{\delta_1}\right)} \tag{11}$$

4.1.2 Neural Structural Control

Another possibility is to use an unsupervised RBFNN to dampen tower motions. Vibrations can be dampened by relating the tower acceleration, Acc_{tt}, to the electromagnetic torque and using the network to solve this relationship. Equations (12) - (14) describe the application of the RBFNN using the tower top acceleration, Acc_{tt}, and its derivative, $A\dot{c}c_{tt}$. As in the speed control, in this vibration control the width of neurons, δ_2, the constants K_3 and K_4 that favor the error reduction, and the learning constant, μ_2, are involved. Finally, in (13) the electromagnetic torque of reference, Tem_{ref2}, is obtained.

$$\|(Acc_{tt}, A\dot{c}c_{tt}, i)\| = \sqrt{\frac{(c_{i1} - Acc_{tt})^2}{Max(Acc_{tt})^2} + \frac{\left(c_{i2} - A\dot{c}c_{tt}\right)^2}{Max\left(A\dot{c}c_{tt}\right)^2}} \tag{12}$$

$$Tem_{ref2} = \sum_{i=1}^{N_2} W_i \cdot e^{-\left(\frac{\|(Acc_{tt}, A\dot{c}c_{tt}, i)\|}{\delta_2}\right)} \tag{13}$$

$$\Delta W_i(t) = -\mu_2\left[Acc_{tt}K_3 + A\dot{c}c_{tt}K_4\right] \cdot e^{-\left(\frac{\|(Acc_{tt}, A\dot{c}c_{tt}, i)\|}{\delta_2}\right)} \tag{14}$$

4.2 PID Controllers for Wind Energy Converters

Although the conventional PID controller have some limitations with non-linear systems such as the wind turbine, it may provide good performance when combined with other techniques. In this work, we have evaluated the use of the PID as a speed regulator and to reduce vibrations, as a member of a combined architecture: PID-NN, NN-PID, PID-PID.

4.2.1 PID Generator Speed Control of the FOWT

The PID speed control of the wind turbine can be implemented to connect generator speed and torque. It requires the calculation of the error speed, and the derivative and the integral of this error. Then the three tuning parameters, proportional K_{p1}, derivate K_{d1} and integral K_{i1} gains have to be adjusted. The PID speed control formula is shown in (15), where the electromagnetic torque Tem_{ref} is estimated.

$$Tem_{ref1} = K_{p1} e\omega_g(t) + K_{i1} \int_0^t e\omega_g(t)\, dt + K_{d1} \frac{d[e\omega_g(t)]}{dt} \tag{15}$$

4.2.2 PID Vibration Control of the FOWT

For vibration control, the PID can also be used, considering the tower acceleration as an error signal. The output torque Tem_{ref2} is calculated in (16), using the tuning gains K_{p2}, K_{i2}, and K_{d2}. The minus sign in the equation is due to the expected acceleration is zero and thus the error is $-Acc_{tt}$.

$$Tem_{ref2} = -K_{p2} Acc_{tt}(t) - K_{i2} \int_0^t Acc_{tt}(t)\, dt - K_{d2} \frac{d[Acc_{tt}(t)]}{dt} \tag{16}$$

4.3 Controllers based on the Hybrid Control Architecture

Based on the proposed hybrid control architecture various possible MPPT controllers can be implemented combining the conventional and intelligent techniques previously explained. Each technique (neural and conventional) can be applied to each of the two system controls: the speed controller and the vibration controller, resulting in four different configurations. The outputs of both of both system controls are added to obtain the final reference torque that must be induced in the machine. In this way the double objective of control is achieved.

The DSC scheme is used to estimate the reference speed $Ref\omega_g$. Based on this reference the speed error signal is obtained. To compute this reference, the main mechanical variables of the turbine that influence the transmission of movement are used: the speed, the torque, and the tip speed ratio, as well as the optimal power coefficient. For vibration control the expected acceleration is zero since it is intended to be eliminated.

By implementing this hybrid control scheme, four control configurations combining PID and RBFNN controllers are created, namely: RBFNN-PID, PID-RBFNN, PID-PID and RBFNN-RBFNN, as shown in Figure 5.

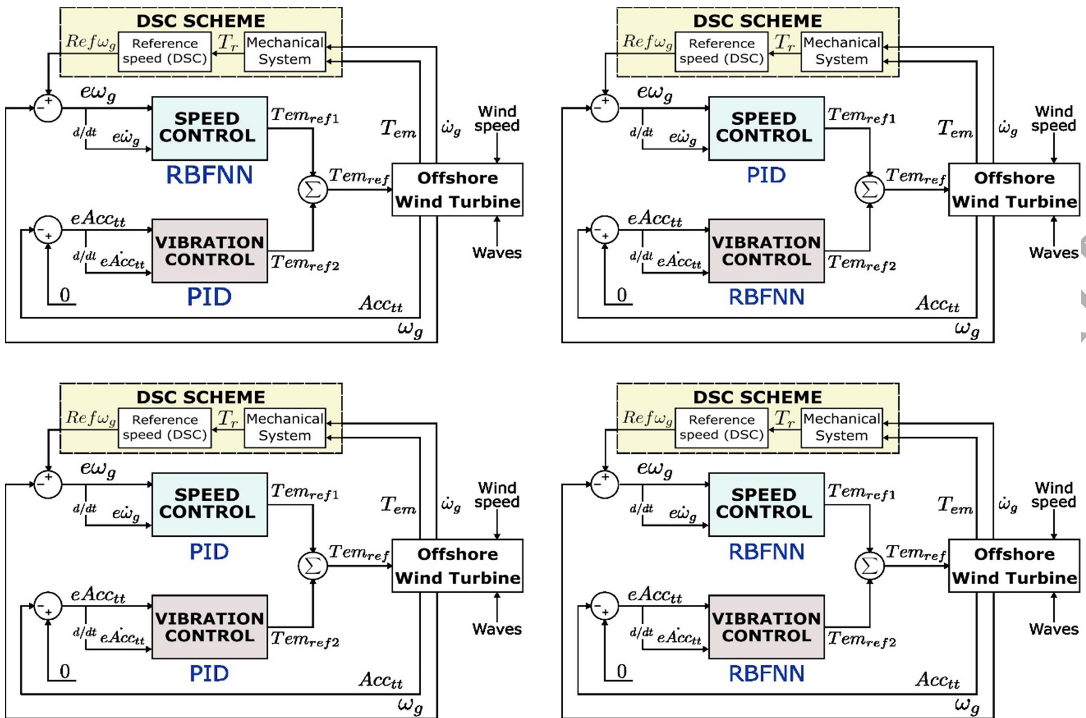

Figure 5. Controllers based on the Hybrid Control Architecture.

5. Optimization of the Control Strategy

For the design of controllers, an important aspect is the adjustment of their parameters. The effectiveness of the control for a given system depends on it. In this case, the parameters have been adjusted using a heuristic optimization technique, Genetic Algorithms (GA), which have proven in the literature to be very useful tools and allow incorporating several criteria in the cost function.

The optimization seeks to minimize a cost function, in our case to reduce an error signal. The cost function will be the normalized Mean Absolute Error (MAE). This metric is used to tune the two controllers with two genetic algorithms. For the speed regulator in the MPPT region, the normalized MAE of the generator speed, MAE_{ω_g} (17), is used.

$$MAE_{\omega_g} = \frac{1}{n \cdot Max(|\omega_g - Ref\omega_g|)} \cdot \sum_{i=1}^{n} |\omega_g - Ref\omega_g| \quad (17)$$

Once the speed controller is tuned, a second genetic algorithm is applied to the vibration controller. The cost function is the normalized MAE of the tower top acceleration signal, $MAE_{Acc_{tt}}$ (18), to reduce or eliminate that acceleration Acc_{tt}.

$$MAE_{Acc_{tt}} = \frac{1}{m \cdot Max(|Acc_{tt}|)} \cdot \sum_{i=1}^{m} |Acc_{tt}| \quad (18)$$

The configuration of the GAs, which have been implemented using the Matlab tool, is as follows. The initial population, of 200 individuals, is initialized randomly. The crossover probability is 0.8. The mutation rate is 0.2. The elite size is set to 5%. The chromosomes, parameters to be optimized, of the neural network for speed control are $[\mathrm{N}_1, \mathrm{K}_1, \mathrm{K}_2, \mu_1, \delta_1, T_c]$, while the gains for the PID controller are $[\mathrm{K}_{\mathrm{p}1}, \mathrm{K}_{\mathrm{i}1}, \mathrm{K}_{d1}]$. For the vibration controller, the tuning coefficients are $[\mathrm{N}_1, \mathrm{K}_1, \mathrm{K}_2, \mu_1, \delta_1, T_c]$ for the RBFNN, and $[\mathrm{K}_{\mathrm{p}2}, \mathrm{K}_{\mathrm{i}2}, \mathrm{K}_{d2}]$ for the PID. The only restriction is that they are values greater than zero.

The procedure to optimize the hybrid controller is summarized in Algorithm 1. *execSimulationSC()* indicates that the simulation is run only with the speed controller (the vibration controller is deactivated), *execSimulationSCVC()* indicates that the simulation is run with the speed controller and the vibration controller. The output of the process is the couple of sets *best_speed_con_coeff* and *best_vibration_con_coeff*, that denote the set of coefficients of the speed controller and the vibration controller, respectively. As explained the size of each one of these sets depend on the type of controller used, when RBFNN is used the size is 6, when PID is used the size is 3.

Algorithm 1 Pseudocode of the optimization of the hybrid controller

Output: {*best_speed_con_coeff*, *best_vibration_con_coeff* }
// speed_controller, RBFNN or PID
initialize: *speed_con_coeff* *//random*
best_speed_con_coeff ← *speed_con_coeff*
while *best_speed_con_coeff unchanged* *//after 50 iterations (i)*
  $[\omega_g, Ref\,\omega_g]$ ← *execSimulationSC*(*speed_con_coeff*)
  $MAE_{\omega_a}(i) \leftarrow MAE_{\omega_a}(\omega_g, Ref\,\omega_g)$
  if $MAE_{\omega_a}(i) < bestMAE_{\omega_a}$
    $bestMAE_{\omega_a} \leftarrow MAE_{\omega_a}$
    best_speed_con_coeff ← *speed_con_coeff*
  End
  speed_con_coeff ← ***Next*** *speed_con_coeff*
End
// vibration_controller, RBFNN or PID
initialize: *vibration_con_coeff* *//random*
best_vibration_con_coeff ← *vibration_con_coeff*
while *best_vibration_con_coeff unchanged* *//after 50 iterations (i)*
  $[Acc_{tt}]$ ← *execSimulationSCVC*(*speed_con_coeff, vibration_con_coeff*)
  $MAE_{Acc_{tt}}(i) \leftarrow MAE_{Acc_{tt}}(Acc_{tt})$
  if $MAE_{Acc_{tt}}(i) < bestMAE_{Acc_{tt}}$
    best$MAE_{Acc_{tt}} \leftarrow MAE_{Acc_{tt}}(i)$
    best_vibration_con_coeff ← *vibration_con_coeff*
    End
    vibration_con_coeff ← ***Next*** *vibration_con_coeff*
  End

In this framework, the four hybrid controllers are designed and optimized for the MPPT and vibration attenuation purposes.

6. Simulation Setup

The main offshore wind turbine characteristics that are used in the simulated model are presented in Table 1, extracted from OpenFAST software and Jonkman et al. (2009).

Table 1. Parameters of the floating wind turbine

Parameters	Values
Model	Offshore floating barge
Number of Blades	3
Rotor radius	63 m
Rated power	5 MW
Rated speed	1200 rpm
Tower height	87.6 m
Gearbox ratio	97
Maximum Tip speed ratio	7.59
Maximum Power coefficient	0.47
Nominal wind speed	11.5 m/s

In order to apply the hybrid controllers to the floating wind turbine, certain environmental conditions of wind and waves have been considered, which are going to directly influence the performance of the device operation in energy production and structural stability. The external conditions used in this work are shown in Figure 6, where Figure 6a illustrates the random wind impinging on the rotor, with a speed range of 8.5 m/s and 11.5 m/s, within the wind turbine partial-load or MPPT region. It constitutes a representative profile to verify the ability of the unsupervised controllers to adapt to different changes of the wind, with which the starting point of a general verification of the control proposal effectiveness is covered, paving the way for more complete and in-depth studies. Figure 6b shows the wave signal with elevations above sea level up to 3.5 m.

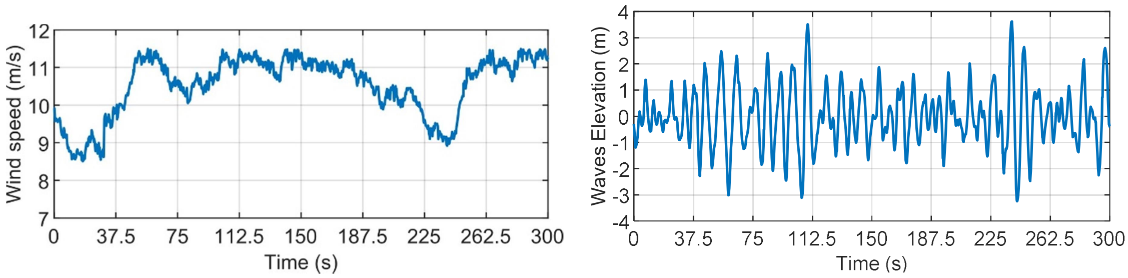

(a) (b)

Figure 6. Input conditions. (a) Wind speed. (b) Waves elevation.

All experiments have been performed starting from the same initial conditions and steady state of the wind turbine. Nevertheless, since the neural networks begin to learn during the first seconds of simulation, the results omit the first 50 seconds of simulation until the networks learn and the neuro controllers can reflect a proper control response.

7. Simulation Results

In the following sections each combination of controller: RBFNN-PID, PID-RBFNN, RBFNN-RBFNN, PID-PID is compared with the results provided by the controller embedded in OpenFast, and also with the implementation of the single MPPT control using RBFNN or PID. Figures 7-10 show this comparison. The power, the generator speed, the power coefficient, and the acceleration of the tower are used as comparison signals. In addition, a table with the parameters of the controller is shown for each configuration.

7.1 Results of the Hybrid RBFNN-PID Control Approach

In this control configuration, neuro-control and PID are used. The RBFNN is applied for the speed controller, while the PID performs the vibration control. After tuning the parameters using GA, the final values are presented in Table 2.

Table 2. Configuration of the RBFNN-PID hybrid control

	Parameters	**RBFNN-PID**	
		Controller 1: MPPT	**Controller 2: Vibrations**
Configuration	K_1	0.7095175	---

RBFNN	K_2	0.3500488	---
	μ_1	0.136155	---
	δ_1	0.3064188	---
	N_1	81	---
	T_c (s)	0.049	---
Configuration PID	K_{p2}	---	0.532749
	K_{d2}	---	1.611950
	K_{i2}	---	0.380332

The results using this hybrid control scheme are shown in Figure 7 and are compared to the OpenFAST speed-torque controller and single RBFNN controller as references. It is possible to observe how the power when the RBFNN-PID is used is larger and the amplitude of the vibrations is smaller than the OpenFAST controller, but the behaviour of the system is slightly inferior compared to the simple neuro controller. The addition of a PID helps to reduce the acceleration magnitude of the tower movement but the output power is affected.

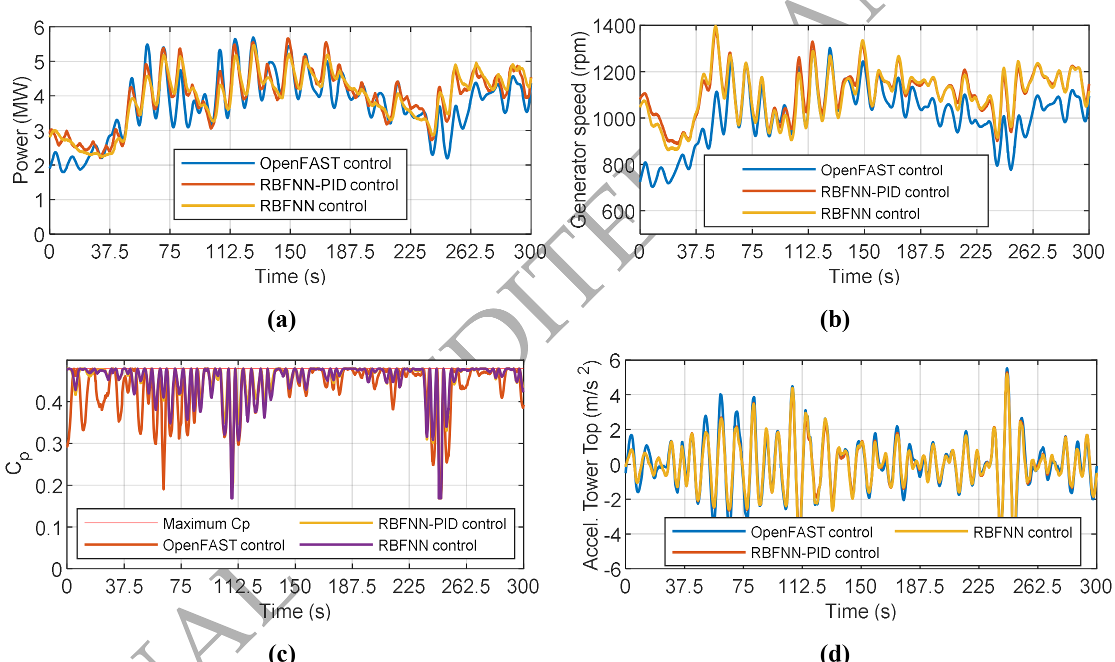

Figure 7. Results with the RBFNN-PID hybrid control scheme.

7.2 Results of the Hybrid PID-RBFNN Control Approach

Applying the same techniques but using in this case a PID for the speed regulator and the neural network for the attenuation of the tower movement, the configuration of the controllers is shown in Table 3 once tuned with genetic algorithms.

With this control architecture, the offshore wind turbine system is simulated. Figure 8 shows the performance results of the proposed controllers vs the response of the floating wind turbine with the control embedded in OpenFAST. As in the previous case it is possible to observe that the amplitude of the vibrations and the oscillatory response of the system are smaller when the hybrid controller is used, even more than the simple PID controller, however, related only to the PID controller, the average power is not increased but the performance of the overall signal is acceptable to maintain the energy without significant changes.

Table 3. Configuration of the PID-RBFNN hybrid control

	Parameters	PID-RBFNN	
		Controller 1: MPPT	**Controller 2: Vibrations**
Configuration RBFNN	K_3	---	7.093677
	K_4	---	6.892176
	μ_2	---	0.575251
	δ_2	---	0.258138
	N_2	---	169
	T_c (s)	---	0.044
Configuration PID	K_{p1}	1.502982	---
	K_{d1}	0.581712	---
	K_{i1}	1.436110	---

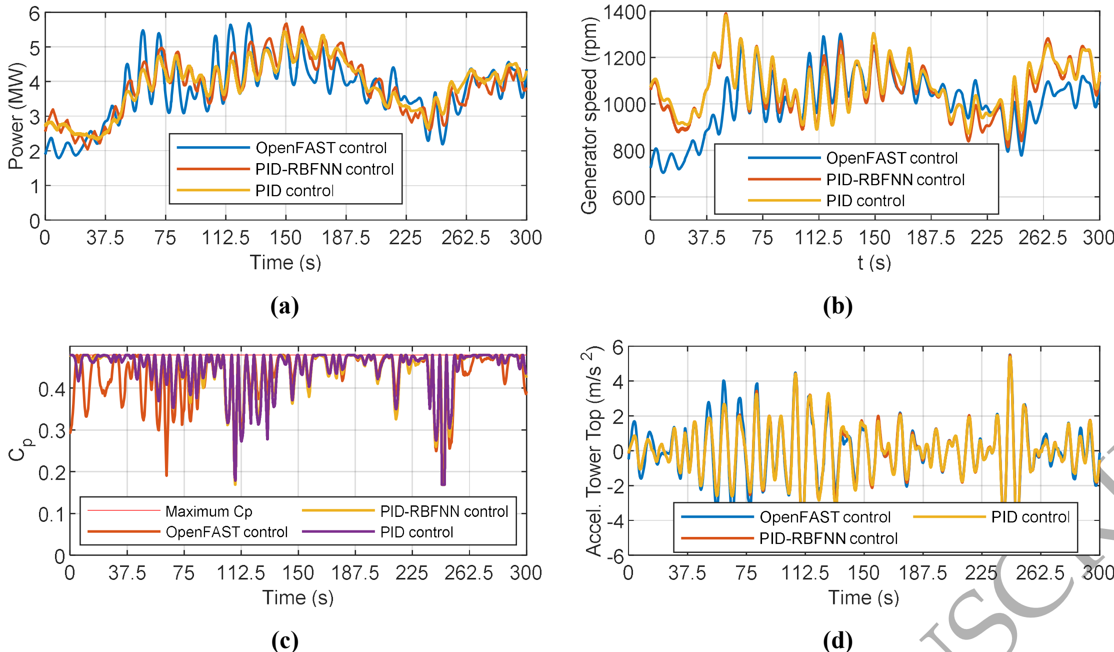

Figure 8. Results with the PID-RBFNN hybrid control scheme.

7.3 Results of the Hybrid PID-PID Control Approach

Using the same type of controller for both objectives, in this case two PIDs, the coefficients found by the genetic algorithms are shown in Table 4. Figure 9 presents the turbine output signals with two conventional controllers for speed and vibrations. As in the previous case the amplitude of the vibrations is smaller when the hybrid controller is used, and the power is less oscillating.

Table 4. Configuration of the PID-PID hybrid control

	Parameters		PID-PID Controller 1: MPPT	PID-PID Controller 2: Vibrations
Configuration PID	K_{p1}	K_{p2}	1.502982	1.207383
	K_{d1}	K_{d2}	0.581712	1.468069
	K_{i1}	K_{i2}	1.436110	0.283085

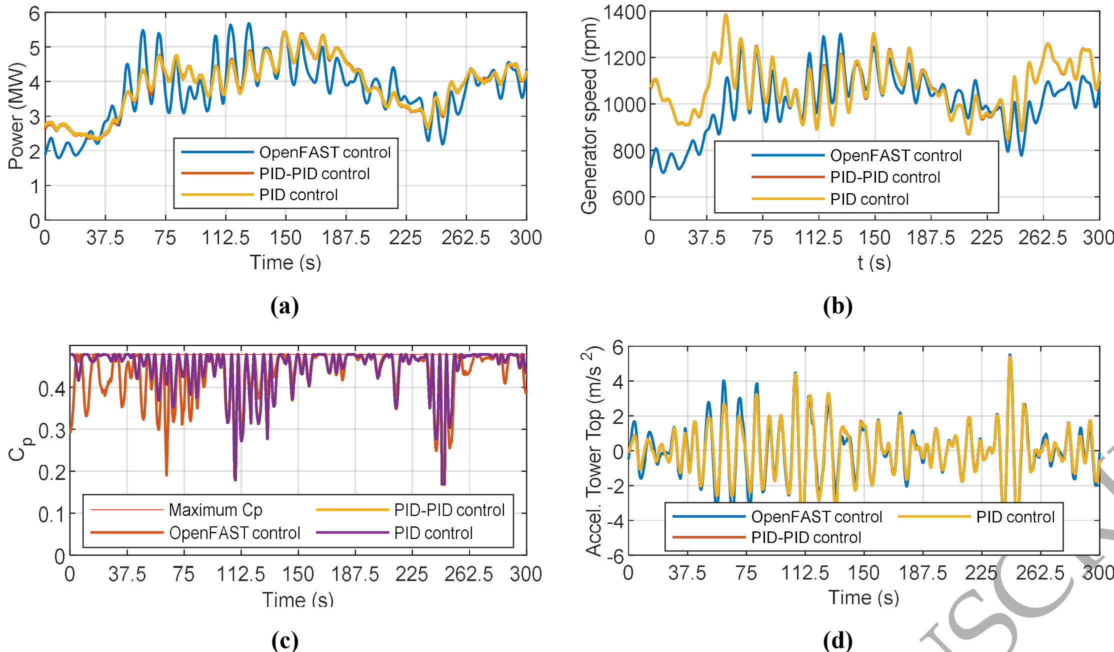

Figure 9. Results with the PID-PID hybrid control scheme.

7.4 Results of the Hybrid RBFNN-RBFNN Control Approach

Finally, the last control combination consists of using two intelligent controllers based on neural networks. The parameters optimized by GA are presented in Table 5. The implementation of the double neural controller is shown in the response of the floating wind turbine shown in Figure 10. In this case the average power is larger, especially when big dynamic changes are introduced, and the vibrations are smaller when the hybrid controller is used.

Table 5. Configuration of the hybrid RBFNN-RBFNN control

	Parameters		RBFNN-RBFNN	
			Controller 1: MPPT	**Controller 2: Vibrations**
Configuration RBFNN	K_1	K_3	0.7095175	48.97649
	K_2	K_4	0.3500488	12.99071
	μ_1	μ_2	0.136155	0.0760591
	δ_1	δ_2	0.3064188	0.3064188
	N_1	N_2	81	121
	T_c (s)	T_c (s)	0.049	0.049

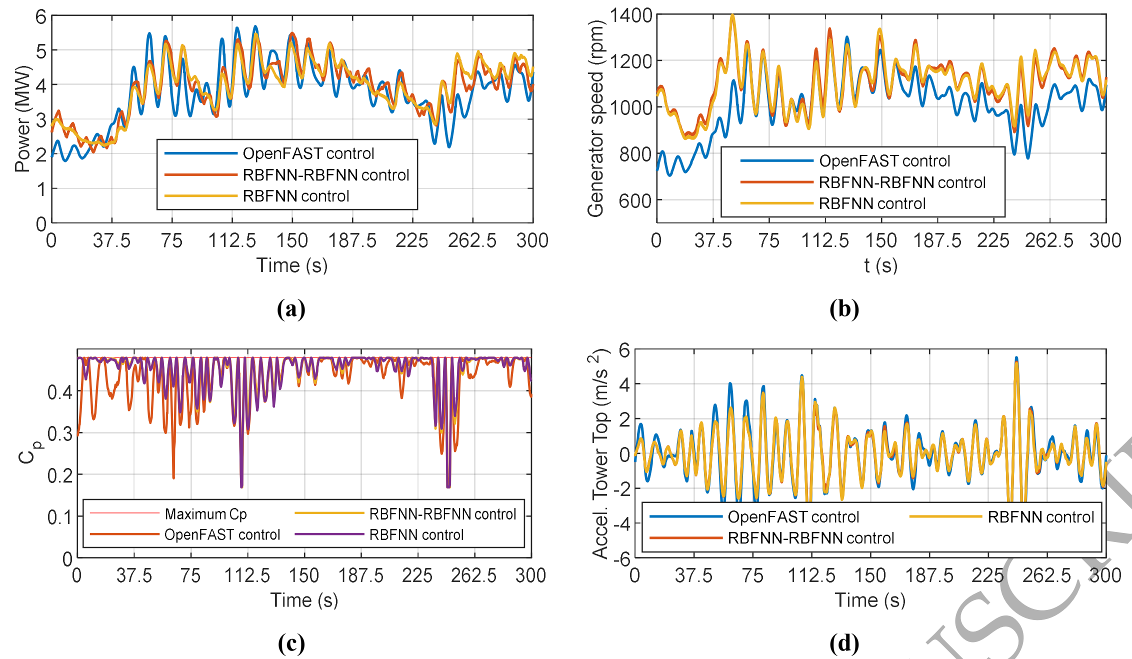

Figure 10. Results with the RBFNN-RBFNN hybrid control scheme.

7.5 Comparison of the different control approaches

The results of hybrid control schemes using PIDs and RBFNNs, as well as the application of only a PID, only RBFNN, and the implementation of OpenFAST for maximum power tracking, are presented in Figures 11-16. The individual controllers provide a general framework for evaluating the advantages and disadvantages of each technique. The colour code is as follows. OpenFAST (blue), RBFNN (red), PID (green), RBFNN-PID (purple), PID-RBFNN (cyan), PID-PID (brown), RBFNN-RBFNN (orange).

The power signal in Figure 11 shows that the RBFNN-based speed control exhibits behaviour with changes that correspond to the dynamic variations of the floating wind turbine and the input conditions. The generator speed, Figure 12, respond to these changes as well. The wind turbine with the neuro-controllers moves with a higher angular velocity than either the PID or the OpenFAST speed regulators. With this performance, the high speed ranges are exploited by the system to reach and oscillate around the optimal TSR and power coefficient, as shown in Figure 13, and thus to track the maximum power.

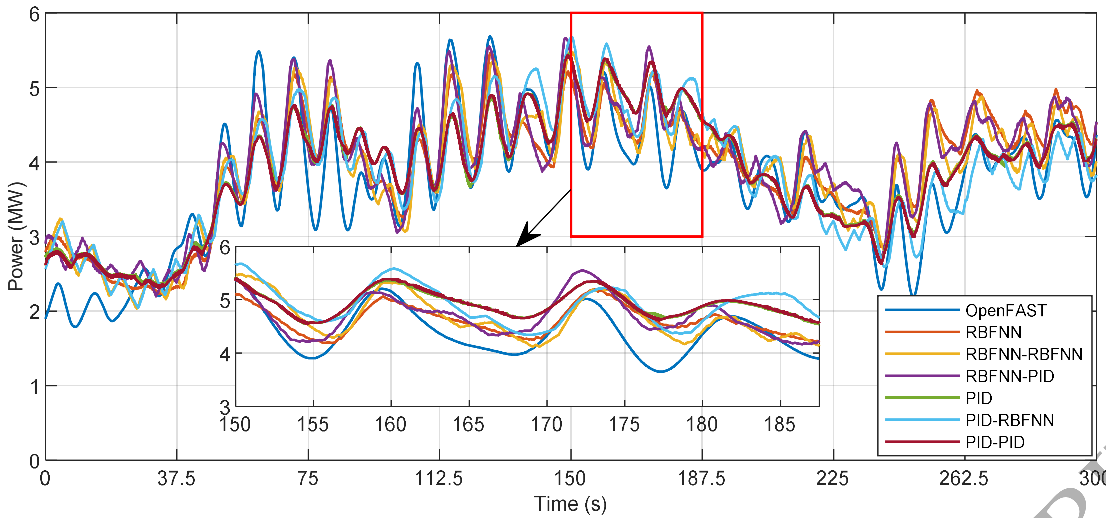

Figure 11. Comparative results of the hybrid control schemes. Power.

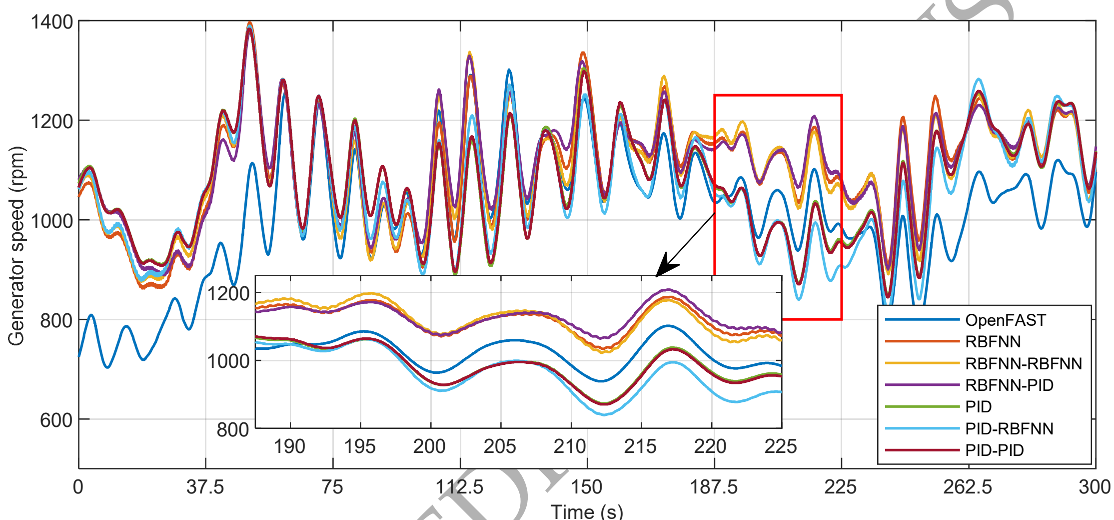

Figure 12. Comparative results of the hybrid control schemes. Generator speed

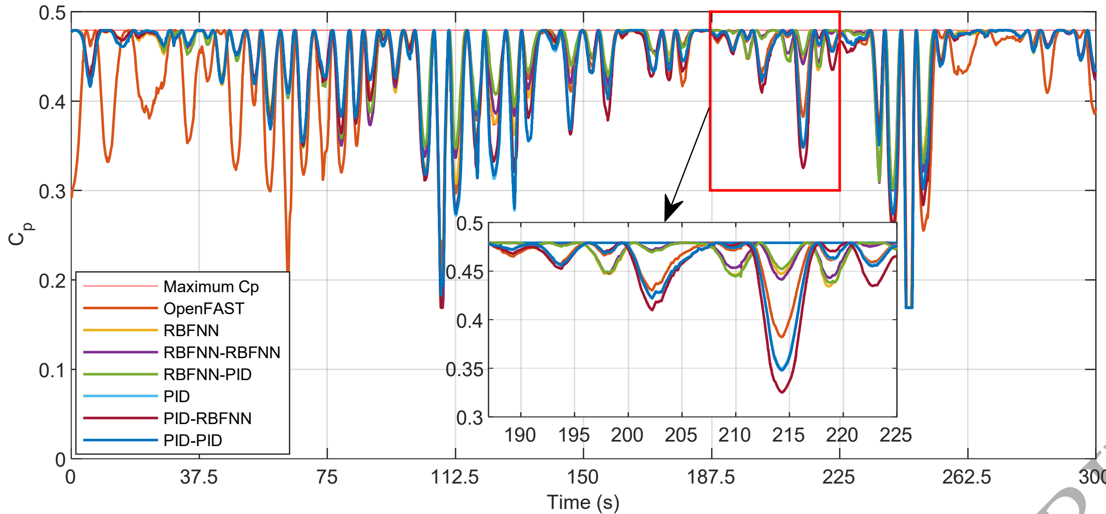

Figure 13. Comparative results of the hybrid control schemes. Power Coefficient

Regarding the second control objective, the structural stability of the wind turbine is analysed based on the movements generated at the top of the tower. The tower top displacement (TTD) is shown in Figure 14, and the acceleration at that point is illustrated in Figure 15. The TTD metric shows the response of the system with minor oscillations and abrupt changes in the structure motion, especially with the RBFNN-based methods for vibration control. Although the mean displacement measured with the different controllers shows that the PID-RBFNN option is the solution with the smallest mean deviation, with a value of 0.355 m, the RBFNN-RBFNN strategy with mean displacements of 0.365 m produces less oscillations. The latter approach has the minimum standard deviation and the minimum root mean square error with the values 0.437 m and 0.324 m^2, respectively. They are followed by the RBFNN-PID and finally the PID speed regulation based controllers.

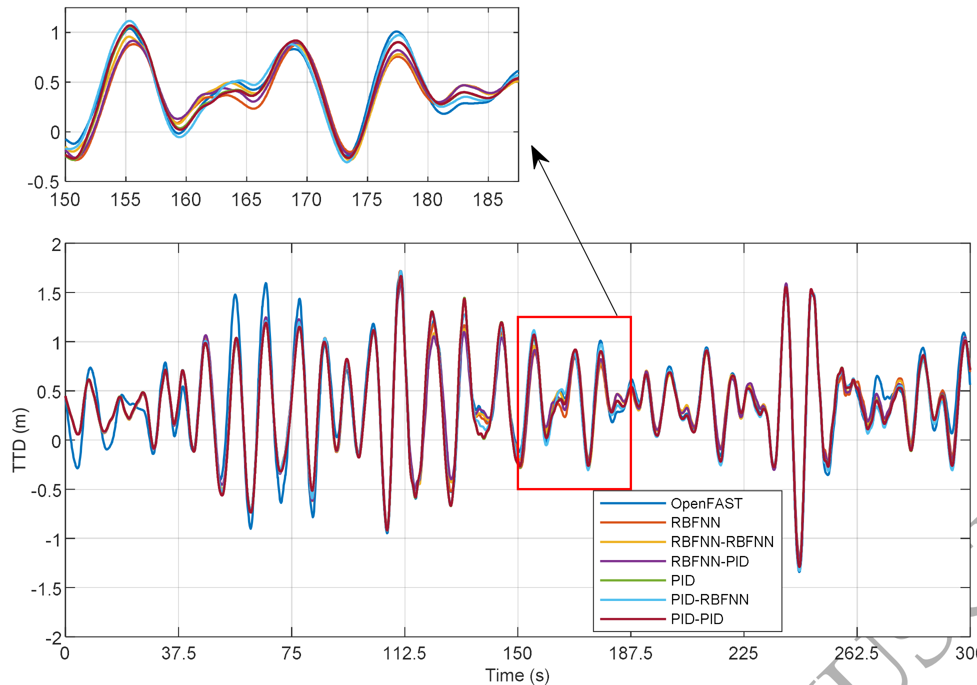

Figure 14. Comparative results of the hybrid control schemes. Tower Top Displacement

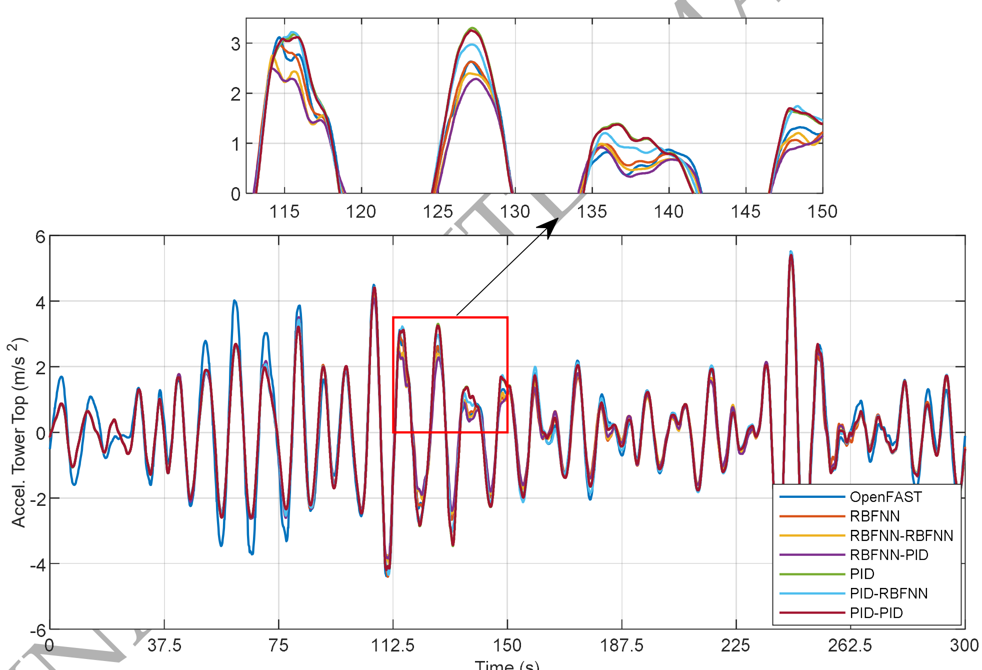

Figure 15. Comparative results of the hybrid control schemes. Tower acceleration

In Figure 16, the frequency spectrum of the vibration clarifies the effects of the different hybrid control strategies. It is shown how the RBFNN-RBFNN approach has the lowest amplitude in the peaks of the spectrum, which are reduced with this controller, followed by RBFNN-only, speed PID and OpenFAST controllers. This reduction is noticeable at frequencies around 0.07 Hz and 0.15 Hz.

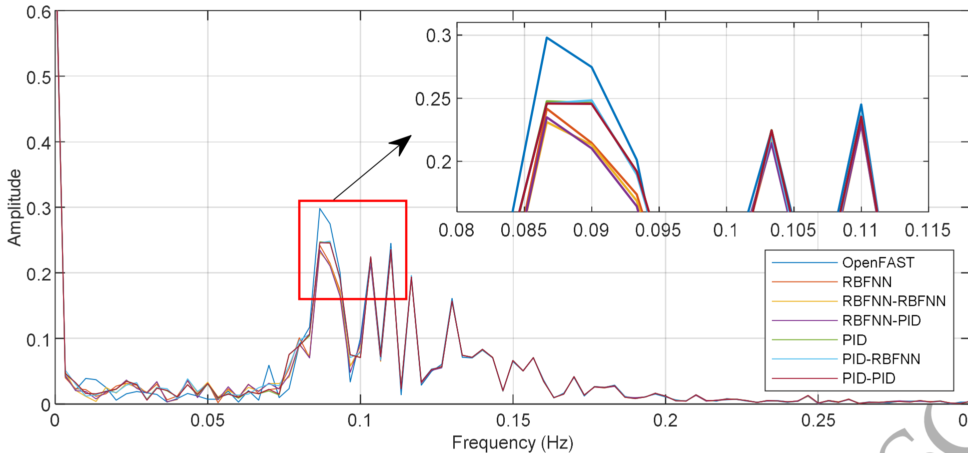

Figure 16. Comparative results of the hybrid control schemes. Frequency spectrum of the TTD

Additionally, the performance metrics are presented in Table 6. These performance indicators during wind turbine MPPT operation analyse the maximization of energy production and the minimization of structural movements.

The average metrics are calculated with Equation (19), where X corresponds to the analyzed variable and T_{sim} is the total simulation time. The suppression rate γ (20) shows the percentage of reduction of the tower top displacement with the control approaches, using the corresponding OpenFAST reference signals. The standard deviation, SD, of the OpenFAST signal is $\sigma_{OpenFAST}$, whereas the standard deviation of the control strategy that is being studied is $\sigma_{controller}$.

$$X_{Avg} = \frac{1}{T_{sim}} \int X_{out}(t) \cdot dt \tag{19}$$

$$X_{\gamma} = \frac{\sigma_{OpenFAST} - \sigma_{controller}}{\sigma_{OpenFAST}} \cdot 100\% \tag{20}$$

According to the results of Table 6, the power conversion is higher on average when any RBFNN is involved in the MPPT control. The neural network alone generates the highest power output of 3.946 MW, followed by the dual RBFNN scheme, where 3.943 MW is produced. This efficiency in power production is reflected in the power coefficient metric, which reaches higher values with these controllers. On the other hand, with the PID-based speed controllers, a reduction in the average power generated is reflected, from 3.891 MW with only speed control to 3.886 MW with the PID-PID approach. The standard deviation of this variable shows an inverse response, giving the neural networks a small increment compared to the PID responses.

Regarding the top tower acceleration, the dual RBFNN controller responds with minimal variation of this signal compared to the other hybrid techniques tested. Moreover, the average acceleration is low, with a value of 0.0040 m/s^2, in contrast to the values of 0.0045 m/s^2, 0.0052 m/s^2, and 0.0055 m/s^2 obtained with the RBFNN-PID, PID-RBFNN and PID-PID controllers, respectively. This means a decrease of 0.0015 m/s^2 from the highest acceleration. This acceleration attenuation is corroborated by the corresponding standard deviation and root mean square error. The smallest values are achieved with the dual neural network, 1.381 m/s^2 and 1.908 m^2/s^4, respectively, while the maximum indicators correspond to 1.481 m/s^2 and 2.189 m^2/s^4 with the speed PID controllers.

With these indicators and based on the vibration suppression capacity in the structure, the RBFNN-RBFNN control technique is the best option. The TTD suppression rate, calculated with respect to the OpenFAST response, achieves the highest reduction of 10.662% with the dual RBFNN. Similarly, the suppression rate of the acceleration at the top of the tower is 12.771% with this control scheme.

Table 6. Numerical results of the hybrid control architectures

Parameters	OpenFAST Control speed-torque	RBFNN	RBFNN-RBFNN	RBFNN-PID	PID	PID-RBFNN	PID-PID
Average Power [MW]	3.75740	<u>**3.94610**</u>	3.94360	3.91900	3.89140	3.86970	3.88600
Power with hybrid controller over OpenFAST [%]	---	<u>5.02050</u>	4.95560	4.30070	3.56430	2.98770	3.42180
Standard Deviation of Power [MW]	0.88695	0.78393	0.79229	0.76862	<u>**0.76619**</u>	0.82154	0.77548
Average C_p	0.43312	0.45044	<u>**0.45144**</u>	0.45008	0.44494	0.44364	0.44502
Average TTD [m]	0.37299	0.36540	0.36517	0.36261	0.35866	<u>**0.35584**</u>	0.35819
TTD with hybrid controller over OpenFAST [%]	---	-2.03440	-2.09680	-2.78160	-3.84250	<u>-4.59650</u>	-3.96830
MSE of TTD [m^2]	0.37846	0.32916	<u>**0.32436**</u>	0.32893	0.34276	0.34121	0.34227
MSE of TTD with hybrid controller over OpenFAST [%]	---	-13.02720	<u>-14.29450</u>	-13.08820	-9.43190	-9.84240	-9.56180
Standard Deviation of TTD [m]	0.48922	0.44232	<u>**0.43706**</u>	0.44435	0.46275	0.46321	0.46257
Suppression Rate of TTD [%]	---	9.58740	<u>**10.66290**</u>	9.17300	5.41160	5.31740	5.44870
Average of Tower Top Acceleration [m/s^2]	0.00938	0.00469	<u>**0.00401**</u>	0.00458	0.00561	0.00525	0.00558
Tower Top Acceleration with hybrid controller over OpenFAST [%]	---	-50.03310	<u>-57.26370</u>	-51.24240	-40.21560	-44.03020	-40.49250
MSE of Tower Top Acceleration [m^2/s^4]	2.50850	1.96850	<u>**1.90860**</u>	1.98820	2.19510	2.19430	2.18960
MSE of Tower Top Acceleration with hybrid controller over OpenFAST [%]	---	-21.52500	<u>-23.91380</u>	-20.74250	-12.49100	-12.52630	-12.71370
Standard Deviation of Tower Top Acceleration [m/s^2]	1.58380	1.40300	<u>**1.38150**</u>	1.41000	1.48160	1.48130	1.47970
Suppression Rate of Tower Top Acceleration [%]	---	11.41280	<u>**12.77140**</u>	10.97220	6.45100	6.47150	6.57000

Figure 17 presents a graphical representation of the metrics obtained with each control strategy to show an overview of the responses and their differences. In this representation of the results, all variables are expressed in percentage points. They are calculated as the normalized form of the values from the minimum and maximum values of each signal. To represent the data, considering the maximum points as the best results, the complementary representation of some variables is expressed in the graph.

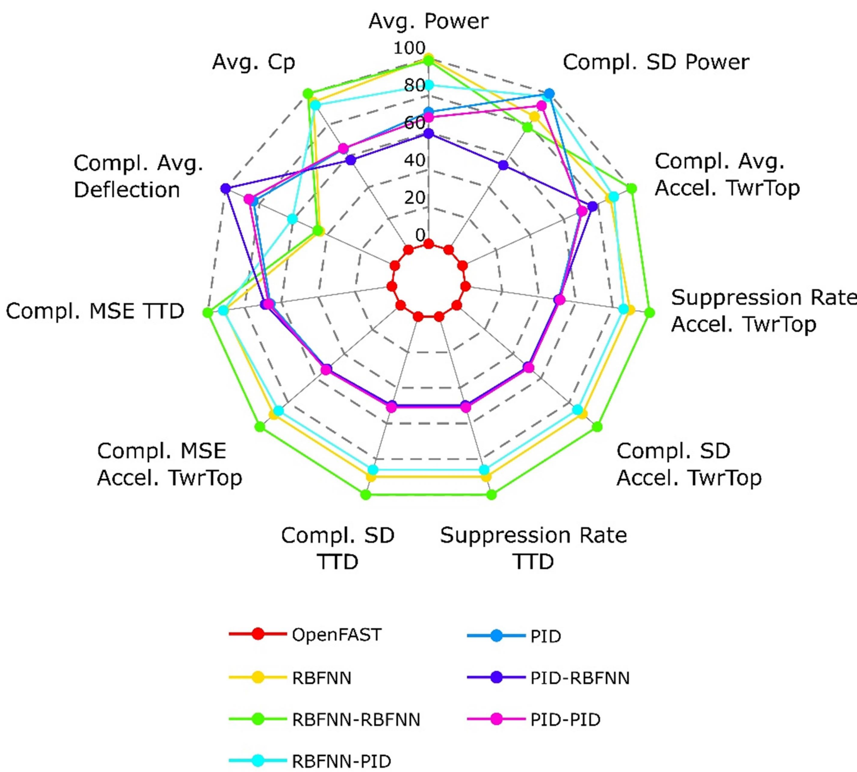

Figure 17. Comparative results of the MPPT control metrics with the different hybrid control schemes

As it can be seen, power performance indicators such as average power and power coefficient acquire the highest values with RBFNN-based strategies in speed control compared to the other hybrid controller approaches, being the most efficient control methods in terms of energy production. On the other hand, PID speed control schemes generate only 60% of the maximum power obtained with RBFNN-based controllers. However, there is a reduction in efficiency with RBFNNs in terms of standard deviation, reaching the minimum value of 80% with RBFNN-RBFNN. The introduction of the PID controller help to reduce the variability.

On the other hand, regarding the stability of the structure measured in terms of reduction of movements and vibrations, it can be observed how the RBFNN-RBFNN control strategy provides a remarkable performance. The SD and MSE of the TTD and all the acceleration metrics of the top of the tower indicate that the neural networks have the highest efficiency in vibration attenuation and acceleration of the tower, while the PID-RBFNN and PID-PID controllers present a decrease of only half.

7.6 Discussion of the Results

Looking at the response of the wind turbine, the wind energy converter reacts directly to environmental conditions, where large changes in wind speed and wave action produce high peaks in the variables, as clearly highlighted at two points around 112.5 and 243 s. The increase in wave amplitude with high wind speed produces, as expected, the largest variations in the response. Considering the generator speed and the power coefficient, thus the TSR, as good indicators of this response, PID controllers generate a behaviour with a higher amplitude of oscillation compared to neural networks. Therefore, the optimal relationship between wind speed and rotor speed is achieved using neuro-controllers.

In this scenario, the electrical torque and simultaneously the output power, have less oscillations around their maximum value with PID controllers, making the generator speed lower to compensate for the movement. With neural controllers, the electromagnetic torque signal presents more variations, following the dynamics of the system and maintaining the rotation speed around the nominal 1200 rpm with the most extreme environmental conditions. Thus, a slightly more oscillatory response in the electrical variables occurs when the neural networks react quickly to small changes in the system dynamics, by adapting the network weights. This behaviour is reflected in the slight increase in the standard deviation of the power signal by 0.01681 MW with the hybrid neuro-controller in the speed and vibration blocks, compared to the dual PID, because the system adapts better to small changes.

In summary, using neural networks, either a RBFNN or dual RBFNN, the highest output power is achieved without the requirement of direct wind speed measurement. A better power coefficient, close to the maximum, is achieved in the MPPT region.

As for structural vibration control, although the average position is lower with PID speed controllers, the oscillations around that point are greater than with RBFNN-based speed control. Therefore, using neuro-controllers the tower maintains a slightly more deviated position, but vibrations and fatigue are reduced. This is because the control action device adjusts the induced torque, so the rotation speed of the generator, and therefore of the turbine rotor, is more stable. Consequently, the acceleration of the tower movement also responds with less oscillations. This is reflected in the higher suppression rate using the dual neural network hybrid controller.

Due to the ability of neural networks to update their weights during wind turbine operation, the controller adapts quickly to dynamic and non-linear changes in the system and is more efficient. This is the main difference with configurations with only PID regulators.

This is reflected in the performance of the different hybrid control proposals. In the proposal, the MPPT objective prevails over vibration reduction, so the approaches with RBFNN in the speed control block (RBFNN-RBFNN and RBFNN-PID) provide higher power, followed by PID MPPT controls (PID-PID and PID-RBFNN).

Similarly, in vibration regulation when speed control is implemented with RBFNN, the motion reduction with RBFNN-RBFNN control is better than with RBFNN-PID. If PID is used for MPPT, the vibration neural network improves the system performance (PID-RBFNN) over PID-PID.

8. Conclusions and Future Works

In this work, several control architectures have been designed and applied for the MPPT region of a floating wind turbine. Conventional PID controllers have been combined with RBFNN neural networks, both for generator speed control and vibration mitigation.

It can be stated that the RBFNN-RBFNN control scheme presents the best performance of all the combinations tested. This approach demonstrates its ability to adapt and respond quickly to external disturbances, achieving maximum power while attenuating structural oscillations. However, conventional PID controllers obtain a lower accuracy in tracking the maximum power point, which leads to a less efficient overall response.

This work opens up new possible lines of research. On the one hand, it would be interesting to apply this dual-objective control approach in the pitch control region of the wind turbine. In addition, the performance of the most promising intelligent control technique can be analysed in more turbulent conditions. To do it, more complex realistic models could be used such as Free Vortex Wake methods, or computational fluid dynamics solutions, to model the hydrodynamics of the environment. Furthermore, the combination of other types of networks and soft computing methods could be explored looking for improvements in the wind turbine regulation. Finally, intelligent control techniques to ensure a trade-off between immediate performance gains and the long-term durability of the turbine could be further researched.

Conflicts of Interest

The authors declare no conflict of interest.

Author Contributions

Eduardo Muñoz-Palomeque: Conceptualization, Methodology, Software, Writing—original draft. **J. Enrique Sierra-García**: Conceptualization, Methodology, Supervision, Writing—review & editing. **Matilde Santos**: Conceptualization, Methodology, Supervision, Writing—review & editing

Acknowledgements

This work is partially supported by the Ministry of Science and Innovation, Spain, with the MICIU/AEI/FEDER project PID2021-123543OB-C21.

References

Aboutalebi, P., M'zoughi, F., Garrido, I., and Garrido, A. J. 2022. "A control technique for hybrid floating offshore wind turbines using oscillating water columns for generated power fluctuation reduction." *Journal of Computational Design and Engineering*, 10(1), 250–265. https://doi.org/10.1093/jcde/qwac137.

Anh Nguyen, Tuan Ngoc, Duy Cong Pham, Luu Hoang Minh, and Nguyen Huu Chan Thanh. 2021. "Combined RBFN Based MPPT and D-Axis Stator Current Control for Permanent Magnet Synchronous Generators." *International Journal of Power*

Electronics and Drive Systems (IJPEDS) 12 (4): 2459. https://doi.org/10.11591/ijpeds.v12.i4.pp2459-2469.

Arianborna, Mohammadhossein, Jawad Faiz, and Amirhossein Erfani-Nik. 2023. "MPPT Control of a PMSG Connected to the Wind Turbine Based on Deep Q-Network." In 2023 *10th Iranian Conference on Renewable Energy & Distributed Generation (ICREDG)*, 1–5. https://doi.org/10.1109/ICREDG58341.2023.10092119.

Atallah, Meddah, Abdelkader Mezouar, Kheira Belgacem, Youcef Saidi, and Mohammed Amine Benmahdjoub. 2022. "Modeling and Control Strategy for a Wind Turbine by an AG-SMC without Wind Speed Sensor." *Journal of Renewable Energies*, June, 9–19. https://doi.org/10.54966/jreen.v1i1.1034.

Chetouani, E., Y. Errami, A. Obbadi, and S. Sahnoun. 2023. "Self-Adapting PI Controller for Grid-Connected DFIG Wind Turbines Based on Recurrent Neural Network Optimization Control under Unbalanced Grid Faults." *Electric Power Systems Research* 214. https://doi.org/10.1016/j.epsr.2022.108829.

Golnary, F., and Tse K.T. 2022. "Simultaneous active control of tower lateral vibration and power control of wind turbine: A novel multivariable approach". *Energy Reports*. 8, pp. 4233-4251. https://doi.org/10.1016/j.egyr.2022.03.083

Gouabi, Hicham, Abdeldjebar Hazzab, Mohamed Habbab, Miloud Rezkallah, and Ambrish Chandra. 2021. "Experimental Implementation of a Novel Scheduling Algorithm for Adaptive and Modified P&O MPPT Controller Using Fuzzy Logic for WECS." *International Journal of Adaptive Control and Signal Processing* 35 (9): 1732–53. https://doi.org/10.1002/acs.3288.

Jonkman, J., S. Butterfield, W. Musial, and G. Scott. 2009. "Definition of a 5-MW Reference Wind Turbine for Offshore System Development." NREL/TP-500-38060, 947422. https://doi.org/10.2172/947422.

Kadri, Ameni, Hajer Marzougui, and Faouzi Bacha. 2019. "Implementation of Direct Power Control Based on Stator Flux Estimation Using Low-Pass Filter Estimator for Doubly Fed Induction Generator–Wind Energy Conversion System." *Proceedings of the Institution of Mechanical Engineers, Part I: Journal of Systems and Control Engineering* 233 (7): 764–78. https://doi.org/10.1177/0959651818818895.

Khan, Mohammad Junaid. 2022. "An AIAPO MPPT Controller Based Real Time Adaptive Maximum Power Point Tracking Technique for Wind Turbine System." *ISA Transactions* 123 (April): 492–504. https://doi.org/10.1016/j.isatra.2021.06.008.

Korlepara, N S D, and Dr. Pragaspathy Subramani. 2022. "Analysis of Dual Stator Winding Induction Generator-Based Wind Energy Conversion System Using Artificial Neural Network Maximum Power Point Tracking." *International Journal of Renewable Energy Research* 12 (March): 372–82. https://doi.org/10.20508/ijrer.v12i1.12759.g8411.

Lara, M., Vázquez, F., Sandua, I., and Garrido, J. 2023a. "Adaptive Active Generator Torque Controller Design Using Multi-Objective Optimization for Tower Lateral Load Reduction in Monopile Offshore Wind Turbines". *IEEE Access*, vol. 11, pp. 115894-115910, 2023, doi: 10.1109/ACCESS.2023.3325840.

Lara, M., Garrido, J., Ruz, M. L., and Vázquez, F. 2023b. "Multi-objective optimization for simultaneously designing active control of tower vibrations and power control in wind turbines". *Energy Reports*, *9*, 1637-1650.

Liu, Hui, Chengqing Yu, Haiping Wu, Zhu Duan, and Guangxi Yan. 2020. "A New Hybrid Ensemble Deep Reinforcement Learning Model for Wind Speed Short Term Forecasting." *Energy* 202 (July): 117794. https://doi.org/10.1016/j.energy.2020.117794.

López-Romero, M. Á., & Peñas, M. S. 2023. "A Positive Position Feedback controller for vibration control of wind turbines". *Energy Reports*, 9, 1342-1353.

Mahmoud, Mohamed Metwally, Mohamed M. Aly, Hossam S. Salama, and Abdel-Moamen M. Abdel-Rahim. 2022. "A Combination of an OTC Based MPPT and Fuzzy Logic Current Control for a Wind-Driven PMSG under Variability of Wind Speed." *Energy Systems* 13 (4): 1075–98. https://doi.org/10.1007/s12667-021-00468-2.

Muñoz-Palomeque, E., Sierra-García, J. E., & Santos, M. 2023a. "Wind turbine maximum power point tracking control based on unsupervised neural networks". *Journal of Computational Design and Engineering*, 10(1), 108-121.

Muñoz-Palomeque, Eduardo, Jesús Enrique Sierra-García, and Matilde Santos. 2023b. "Técnicas de control inteligente para el seguimiento del punto de máxima potencia en turbinas eólicas." *Revista Iberoamericana de Automática e Informática industrial*. https://doi.org/10.4995/riai.2024.21097.

Penta, Samyuktha, S. Venkateshwarlu, and K. Naga Sujatha. 2023. "A Novel Adaptive Controller with Lyapunov Analysis for Strategy Grid Intelligent Integrated Wind Turbine Maximum Power Point Tracking System." *International Journal of Intelligent Systems and Applications in Engineering* 11 (9s): 94–107.

Pinto, Giuseppe, Davide Deltetto, and Alfonso Capozzoli. 2021. "Data-Driven District Energy Management with Surrogate Models and Deep Reinforcement Learning." *Applied Energy* 304 (December): 117642. https://doi.org/10.1016/j.apenergy.2021.117642.

Rahman, M.M. Atiqur, and A.H.M.A. Rahim. 2020. "Design and Testing of an MPPT Algorithm Using an Intelligent RBF Neural Network and Optimum Relation Based Strategy." In *2020 IEEE Region 10 Symposium (TENSYMP)*, 1245–48. Dhaka, Bangladesh: IEEE. https://doi.org/10.1109/TENSYMP50017.2020.9230807.

Salic, Tom, Jean Frédéric Charpentier, Mohamed Benbouzid, and Marc Le Boulluec. 2019. "Control Strategies for Floating Offshore Wind Turbine: Challenges and Trends." *Electronics* 8 (10): 1185. https://doi.org/10.3390/electronics8101185.

Salih, Bashar Mohammed, Khaleel Nawafal, and Safwan Assaf Hamoodi. 2023. "Enhancing the Maximum Power of Wind Turbine Using Artificial Neural Network." *Bulletin of Electrical Engineering and Informatics* 12 (5): 2535–42. https://doi.org/10.11591/eei.v12i5.5019.

Serrano-Antoñanazas, M., Sierra-Garcia, J. E., Santos, M., & Tomas-Rodríguez, M. (2023). Identification of Vibration Modes in Floating Offshore Wind Turbines. Journal of Marine Science and Engineering, 11(10), 1893.

Serrano, C., Sierra-Garcia, J.E. and Santos, M., 2022. "Hybrid optimized fuzzy pitch controller of a floating wind turbine with fatigue analysis". *Journal of Marine Science and Engineering*, 10(11), p.1769.

Sitharthan, R, T Parthasarathy, S Sheeba Rani, and Kc Ramya. 2019. "An Improved Radial Basis Function Neural Network Control Strategy-Based Maximum Power Point Tracking Controller for Wind Power Generation System." *Transactions of the*

Institute of Measurement and Control 41 (11): 3158–70. https://doi.org/10.1177/0142331218823858.

Tsai, Ming-Fa, Chung-Shi Tseng, Yu-Hsiang Hung, and Kuo-Lung Tsai. 2022. "A Novel Digital-Signal-Processor-Based Maximum-Power-Point Tracking Control Design for a Vertical-Axis Wind-Turbine Generation System Using Neural Network Compensator." *IET Electric Power Applications* 16 (7): 761–75. https://doi.org/10.1049/elp2.12190.

Villegas-Mier, César G., Juvenal Rodriguez-Resendiz, José M. Álvarez-Alvarado, Hugo Rodriguez-Resendiz, Ana Marcela Herrera-Navarro, and Omar Rodríguez-Abreo. 2021. "Artificial Neural Networks in MPPT Algorithms for Optimization of Photovoltaic Power Systems: A Review." *Micromachines* 12 (10): 1260. https://doi.org/10.3390/mi12101260.

Wang, L., Wang, L., and Hong, Y. 2024. "Mitigation of side-to-side vibration of a 10MW monopile offshore wind turbine under misaligned wind and wave conditions by an active torque control". *Journal of Sound and Vibration*, 574, 118225.

Wang, J., Golnary, F., Li, S., Weerasuriya, A. U., and Tse, K. T. 2024. "A review on power control of wind turbines with the perspective of dynamic load mitigation". *Ocean Engineering*, 311, 118806.

Zhou, B., Zhang, Z., Li, G., Yang, D., & Santos, M. 2023. "Review of key technologies for offshore floating wind power generation". *Energies*, 16(2), 710.